Responses to the RC #1

To RC #1:

Thank you for your very professional and thoughtful comments. We have followed all your suggestions in our revision. Below are the Reviewer's previous comments, followed by our responses.

RC #1's:

General comments

[RC #1 General comments]

This manuscript introduces a long-term, high-resolution oasis land-cover dataset, which is valuable for understanding the spatio-temporal dynamics of oasis systems and for related environmental and resource management applications.

[Response]

Thank you for your positive comment.

[RC #1 General comments 1]

1. In the introduction section, the overview of current continuous land cover data is not sufficient. Specifically, all land cover datasets mentioned in Section 2.8 lack sufficient description.

[Response]

We thank the reviewer for this helpful comment. In the latest version, we have added an overview of current land cover datasets in the Introduction and provided brief descriptions of the datasets presented in Section 2.8. The detailed revisions are as follows (Lines 48–61 and 188–204):

1 Introduction

Remote sensing technology provides a vital means for monitoring land-cover information (Yang and Huang, 2021). With advancements in satellite and remote sensing technologies, the spatial and temporal resolution of mapping has significantly improved (Tu et al., 2024). In recent years, a series of land-cover datasets with continuous or annual observations have been developed at global and regional scales, greatly improving the capacity to monitor long-term land-cover dynamics. Representative datasets include the Moderate Resolution Imaging Spectroradiometer (MODIS)-based annual land-cover product (MCD12Q1, 500 m) (Sulla-Menashe et al., 2019) and the European Space Agency Climate Change Initiative Land Cover dataset (ESA CCI LC, 300 m) (Defourny et al., 2017). At finer spatial resolution, Landsat-based products include the China Land Cover Dataset (CLCD, 30 m) (Yang and Huang, 2021), the temporally consistent annual land cover maps over China (ALCC, 30 m) (Li et al., 2026), and the Global Land-Cover product with Fine Classification System (GLC_FCS30, 30 m) (Zhang et al., 2021). These datasets have provided important support for land-change studies. However, their application to oasis studies remains limited. Coarse-resolution products are often affected by mixed pixels, making them unsuitable for fine-scale change analysis (Yang and Huang, 2021). Higher-resolution products can better capture spatial details, and several existing datasets have reported good overall accuracy. Nevertheless, these advantages do not necessarily guarantee equally reliable performance in oasis regions because land cover in these regions often shows strong interannual variability.

2.8 Datasets inter-comparison

We compared OasisMap30 with several widely used and well-validated land cover products, including three global datasets, namely MCD12Q1, ESACCI_LC, and GLC_FCS30, with spatial resolutions of 500, 300, and 30 m, respectively (Table S3). We also selected CLCD and ALCC, both of which are annual 30 m land cover datasets for China, with reported overall accuracies of 79.3% and 81.11%, respectively. In addition, we assessed the accuracy of OasisMap30 through inter-comparison with 30 m resolution thematic data derived from Landsat imagery. The current primary impervious surface datasets covering oasis regions include Global Impervious Surface Area (GISA) (Huang et al., 2021) and Global Artificial Impervious Area (GAIA) (Gong et al., 2020). GISA and GAIA provide long-term information on impervious surface dynamics, covering the periods 1972–2021 and 1985–2024, respectively. Crop-related thematic datasets mainly comprise Global Land Analysis & Discovery Cropland Data (GLAD) (Potapov et al., 2021), the Hybrid Cropland Maps of China (CCropland30) (Zhang et al., 2024), and the Annual Cropland Dataset of China (CACD) (Tu et al., 2024). GLAD is a globally consistent cropland dataset covering the period 2000–2019, with maps produced at 4-year intervals. CCropland30 and CACD are cropland distribution datasets for China, covering 2000–2020 with maps produced at 5-year intervals and 1986–2021 with annual maps, respectively. For surface water, the Global Surface Water (GSW) dataset was selected (Pekel et al., 2016), which covers the period 1985–2021. Compared with OasisMap30, GSW provides a much denser temporal record (monthly). To facilitate comparison, we calculated annual mean surface-water extent from the monthly GSW data. These thematic datasets have been shown to have good accuracy in previous studies.

[RC #1 General comments 2]

The validation of land cover dynamics in China's oases from 1987 to 2024 should be clarified.

[Response]

We thank the reviewer for pointing out this issue. In the revised manuscript, we further clarified the validation of land-cover dynamics in China's oases from 1987 to 2024. Specifically, we supplemented the annual accuracy assessment results to show the reliability of the yearly land-cover maps. In addition, as shown in Figure 8, the overall temporal trend of oasis area derived from OasisMap30 is broadly similar to those of other land-cover datasets. The newly added annual accuracy assessment results, together with the comparison between OasisMap30 and other land-cover datasets, help clarify how the long-term land-cover dynamics were validated in this study. The detailed revisions are as follows (Lines 291–294 and Table S4):

Table S4. Pixel-wise accuracy of OasisMap30 calculated based on the annual visually interpreted samples.

Year	OA	Kappa
1987	90.40	0.864
1988	90.43	0.865
1989	90.47	0.867
1990	90.45	0.868
1991	90.51	0.868
1992	90.55	0.866
1993	90.67	0.870
1994	90.71	0.872
1995	90.74	0.871
1996	90.82	0.875
1997	90.91	0.876
1998	91.03	0.878
1999	91.13	0.876
2000	91.12	0.877
2001	91.20	0.876
2002	91.32	0.877
2003	91.47	0.878
2004	91.43	0.879
2005	91.48	0.879
2006	91.59	0.880
2007	91.52	0.881
2008	91.63	0.882
2009	91.67	0.882
2010	91.72	0.882
2011	91.77	0.883
2012	91.82	0.883
2013	91.96	0.883
2014	91.85	0.883
2015	92.04	0.885
2016	92.38	0.886

Table S4 (continued).

Year	OA	Kappa
2017	92.51	0.889
2018	92.90	0.891
2019	92.88	0.890
2020	93.09	0.893
2021	93.34	0.896
2022	93.64	0.899
2023	93.85	0.899
2024	94.05	0.902

Note: OA: overall accuracy; Kappa: Kappa coefficient.

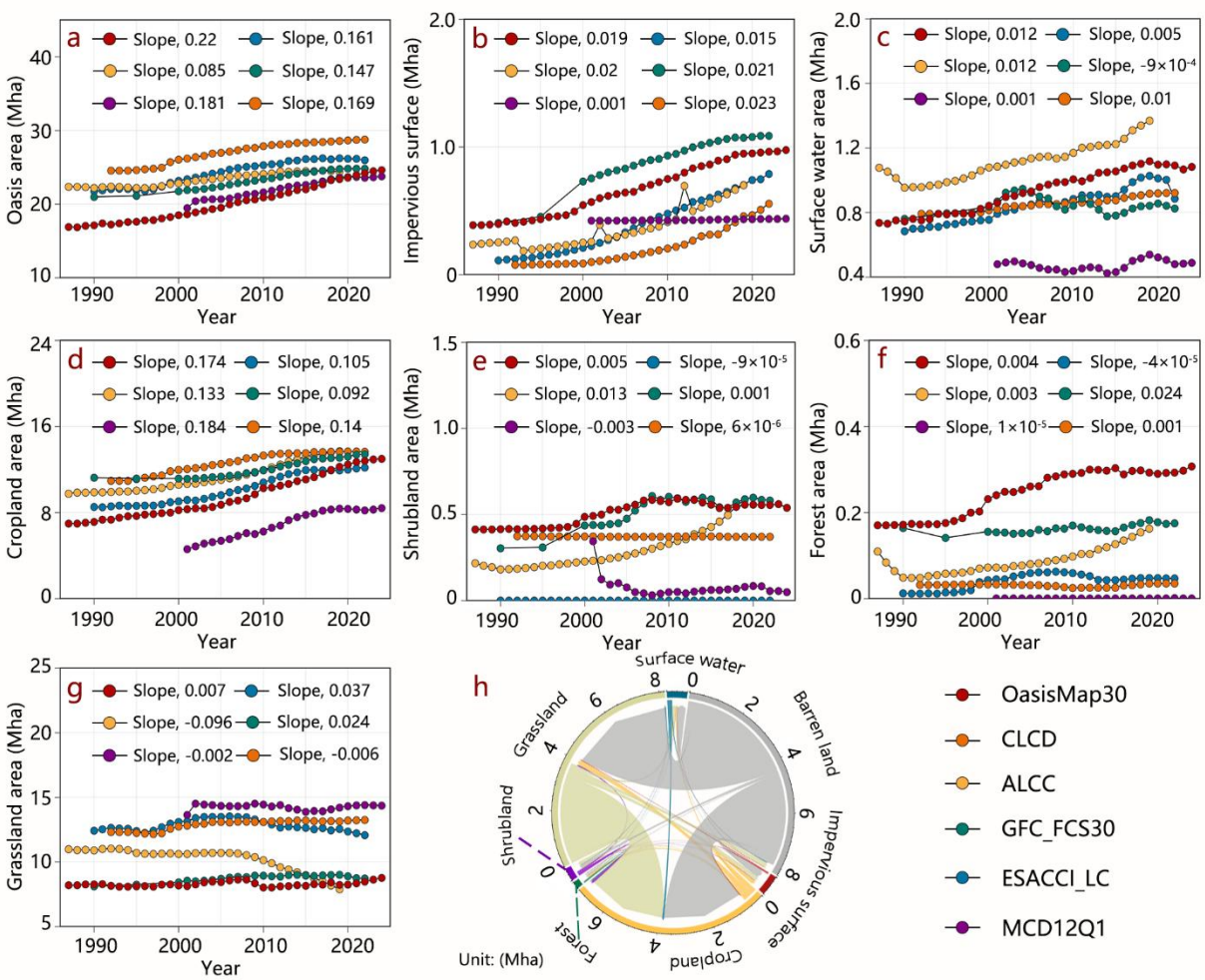

Figure 8: Comparison of temporal changes in different land cover areas of Chinese oases between OasisMap30 and various land cover datasets from 1987 to 2024 (a-g); Changes of seven land cover types during the period of 1987-2024 in oasis of China.

[RC #1 General comments 3]

3. The manuscript applies the LandTrendr algorithm, but key parameter settings (e.g., maximum segments, recovery threshold) are not clearly described in the main text. Please clarify whether default parameters were used or provide the main parameter values.

[Response]

We thank the reviewer for pointing out this issue. We have clarified the parameter settings used for the LandTrendr algorithm in the revised version, and the revised details are as follows (Lines 140–142):

Therefore, to map land-cover dynamics from 1987 to 2024 while limiting the propagation of classification errors, we used the final 2024 oasis land-cover dataset as the baseline map and applied the LandTrendr algorithm to the annual time series of spectral indices, with the main parameter settings provided in Supplementary Table 2.

Table S2 LandTrendr parameter settings

Parameter	Setting	Description
maxSegments	8	Maximum number of segments to be fitted on the time series
spikeThreshold	0.9	Threshold for dampening the spikes (1.0 means no dampening)
vertexCountOvershoot	3	The inital model can overshoot the maxSegments + 1 vertices by this amount. Later, it will be prunned down to maxSegments + 1
preventOneYearRecovery	ture	Prevent segments that represent one year recoveries
recoveryThreshold	0.25	If a segment has a recovery rate faster than 1/recoveryThreshold (in years), then the segment is disallowed
pvalThreshold	0.05	If the p-value of the fitted model exceeds this threshold, then the current model is discarded and another one is fitted using the Levenberg-Marquardt optimizer
bestModelProportion	0.75	Takes the model with most vertices that has a p-value that is at most this proportion away from the model with lowest p-value
minObservationsNeeded	6	Min observations needed to perform output fitting

Specific comments

[RC #1 Specific comments 1]

Line 97 The manuscript states that the tasseled cap transformation was applied using coefficients from Crist et al. (1985). Given that this study uses Landsat 5, 7, and 8 data, the

authors should check and clarify whether the cited coefficients are appropriate for all sensors involved.

[Response]

Thank you for this helpful comment. In this work, different tasseled cap transformation coefficients were used for different Landsat sensors, based on Crist (1985), Huang et al. (2002), and Baig et al. (2014). We have clarified this point in the revised manuscript. The revised text is as follows (Lines 107–110):

Based on Landsat imagery and SRTM DEM data, we derived the predictor variables used in the random forest classification (Breiman, 2001). Among these, slope, aspect, and hillshade were computed from the DEM data. To enhance classification performance, we further applied the tasseled cap transformation to derive brightness, greenness, and wetness components (Crist, 1985; Huang et al., 2002; Baig et al., 2014).

Reference

Baig, M. H. A., Zhang, L., Shuai, T., and Tong, Q.: Derivation of a tasselled cap transformation based on Landsat 8 at-satellite reflectance, Remote Sensing Letters, 5, 423–431, https://doi.org/10.1080/2150704X.2014.915434, 2014.

Crist, E. P.: A TM Tasseled Cap equivalent transformation for reflectance factor data, Remote Sensing of Environment, 17, 301–306, https://doi.org/10.1016/0034-4257(85)90102-6, 1985.

Huang, C., Wylie, B., Yang, L., Homer, C., and Zylstra, G.: Derivation of a tasselled cap transformation based on Landsat 7 at-satellite reflectance, International Journal of Remote Sensing, 23, 1741–1748, https://doi.org/10.1080/01431160110106113, 2002.

[RC #1 Specific comments 2]

Line 126 "…a single composite disturbance metric (MAGPCA)", "PCA" should be a subscript.

[Response]

We thank the reviewer for pointing out this issue and have corrected the formatting accordingly. The details were revised as follows (Lines 146–L147):

We then applied PCA to the disturbance magnitudes of multiple indices to derive a single composite disturbance metric (MAG_{PCA}), …

[RC #1 Specific comments 3]

Line 129 "…we obtained DURmode and YODmode maps", "mode" should be a subscript.

[Response]

We thank the reviewer for pointing out this issue and have corrected the formatting accordingly. The details were revised as follows (Lines 149– L150):

Subsequently, by taking the mode values of DUR and YOD distribution for all indicators, we obtained DUR_{mode} and YOD_{mode} maps, thereby defining the time windows for potential transitions.

[RC #1 Specific comments 4]

Line 136 In Section 2.6, the manuscript describes an evaluation of the dispersion of the detected year-of-disturbance (YOD). However, the results of this analysis (e.g., in figures or tables) are missing. The authors should provide the relevant results to support this analysis.

[Response]

We thank the reviewer for pointing out this issue. Following your suggestion, we have added the results of the YOD dispersion analysis in the revised manuscript. The detailed revisions are as follows (Lines 159–L161):

To verify the accuracy of the disturbance timing identified by this method, we examined the dispersion of the YOD distribution across indices (Eq. 1). The results indicate that $YOD_{indicator}$ exhibits a high degree of consistency (Figure S2).

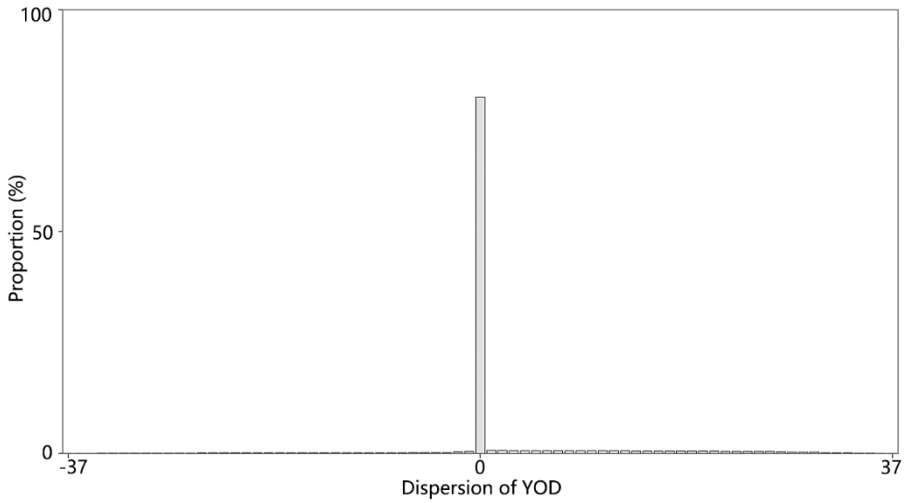

Figure S2. Dispersion of YOD for each indicator based on Landtrendr.

[RC #1 Specific comments 5]

Line 195 The manuscript reports accuracy assessment results, but it is unclear whether the training and validation samples are spatially well distributed across the study area. Additional details on the spatial distribution of the samples should be provided.

[Response]

We thank the reviewer for pointing out this issue. Following your suggestion, we have added further details on the spatial distribution of the samples in the revised manuscript and included a figure showing the spatial distribution of the visually interpreted samples. Specifically, the oasis area was divided into approximately 1100 independent units using regular hexagons with a 10 km side length, and 25 sample points were randomly generated within each unit to ensure spatially uniform sample distribution. After visual interpretation and quality screening, at least 27000 samples were retained for each year. The detailed revisions are as follows (Lines 119–122):

To ensure a spatially uniform distribution of samples across the oasis region, the oasis area was divided into approximately 1100 independent units using regular hexagons with a 10 km side length, and 25 sample points were randomly generated within each unit. After visual interpretation and quality screening, at least 27000

samples were retained for each year (Figure S1).

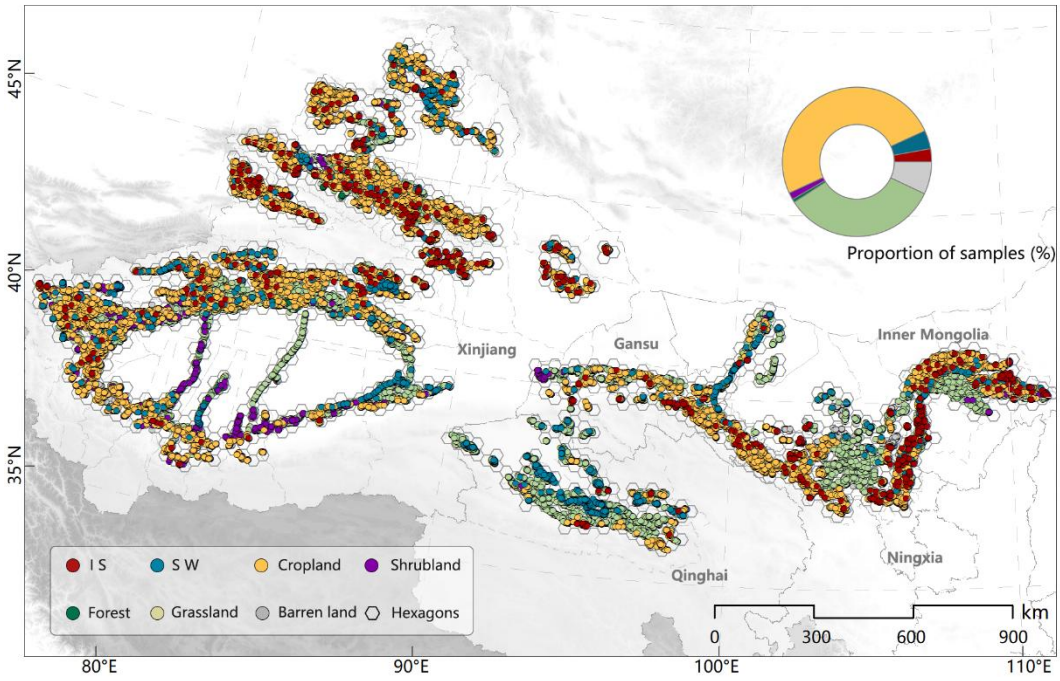

Figure S1. Spatial distribution of validation samples (taking the year 2024 as an example).

[RC #1 Specific comments 6]

Line 321 Grammatical error: “producing a high spatio-temporal resolution land cover datasets for oases are essential …”.

[Response]

Thank you for pointing out this grammatical error. We have revised the sentence accordingly. The revised sentence reads as follows (Lines 370–371):

Given their importance, a high spatio-temporal resolution land cover dataset is essential for understanding patterns of oasis evolution and their ecological impacts.

Response to RC#2

To RC #2:

Thank you for your very professional and thoughtful comments. We have followed all your suggestions in our revision. Below are the Reviewer's previous comments, followed by our responses.

RC #2's:

General comments

[*RC #2 *General comments]

This work produced a valuable datasets on the oasis of China. Generally, the method for data production is reasonable. My concerns mainly related to the basic definition of oasis. The detail comments are given below.

[Response]

Thank you for your positive comment.

[RC #2 General comments 1]

The definition of oasis must be clearly described. The present version of the preprint defined it as "all land-cover types other than barren land". Oasis is a geographical complex of various land cover types including areas with vegetation cover and non vegetation cover. According to the nature of the oasis, it is defined following several criteria at least: (1) located in desert areas; (2) with water sources in the forms such as streams, rivers, ground water, constructed channels et al.;(3) specific plants and other organisms formed azonal vegetated landscape.

[Response]

We appreciate the reviewer's careful comment on this issue. Following the reviewer's suggestion, we have revised the manuscript to clarify the conceptual definition of oasis and to

distinguish it from the operational rule used in our land-cover mapping. In the revised Introduction, we refined the definition of oasis. In the revised Methods section, we now explicitly state that vegetated land-cover types, together with some non-vegetated surfaces, including surface water and impervious surfaces, within the delineated oasis extent, were treated as components of oasis landscapes. The detailed revisions are as follows (Lines 32–35 and 96–99):

1 Introduction

Oases are the most productive and vulnerable landscapes in drylands (Chen et al., 2024a). An oasis is generally defined as a geographical complex formed in arid desert regions, with deserts serving as the surrounding landscape matrix, sustained by relatively stable water resources, characterized by azonal vegetated landscapes, and capable of supporting human activities such as agriculture, animal husbandry, and industrial production (Lin et al., 2024; Zhou et al., 2015).

2.1 Delineation of China's oasis extent

Within this study area, we classified land cover into seven types: impervious surface, surface water, cropland, shrubland, forest, grassland and barren land. Based on the conceptual definition of oasis and the land-cover classification system used in this study, vegetated land-cover types together with surface water and impervious surfaces within the delineated oasis extent were treated as components of oasis landscapes, whereas barren land was excluded.

[RC #2 General comments 2]

In desert areas, the precipitation and the water resources featured with great annual fluctuation. Thus the abrupt change in reflectance may not indicate a change in land cover types. I suggest a caution when use annual indices such as NDVI in mapping, and considered the impacts of climate fluctuation on the accuracy.

[Response]

We thank the reviewer for raising this valuable comment. As the reviewer pointed out, climatic fluctuations in arid regions may influence spectral signals, and abrupt interannual changes in a single index do not necessarily indicate true land-cover change. To reduce this effect, annual land-cover change in our study was not identified directly from anomalies in

any single index. Instead, we used the LandTrendr–PCA framework to integrate disturbance information from multiple indicators, together with visual correction, to reduce classification uncertainty. However, we cannot guarantee that all classification uncertainty caused by climatic fluctuations was fully corrected. Following the reviewer's suggestion, we have also added a discussion in the revised manuscript on the potential impact of climatic fluctuations on mapping accuracy. The detailed revisions are as follows (Lines 323–338):

4.3 Limitations and prospects

… In addition, precipitation and water availability in arid regions often exhibit strong interannual fluctuations, which may affect vegetation and water related spectral signals. As a result, some abrupt spectral changes may not indicate land-cover change. To reduce this effect, we integrated disturbance information from multiple indicators through the LandTrendr–PCA framework rather than relying on abrupt changes in a single index. Nevertheless, climate-driven spectral anomalies may still contribute to uncertainty in annual land-cover mapping. Although visual interpretation helped reduce inevitable land-cover misclassification, complete error correction cannot be guaranteed.

[RC #2 General comments 3]

As to the comparison with other land cover products, resolutions of the land cover products matters. For instance, spatial resolution of MCD12Q1 is 500 m, while ESACCI_LC is 300 m. The comparison with land cover dataset greatly differed in spatial resolution is no sense. What's more, evaluating the accuracy of other datasets using the samples collected for OasisMap30 directly may not reasonable due to the difference in resolution.

[Response]

We thank the reviewer for this helpful comment. We agree that differences in spatial resolution need to be carefully considered when comparing different land cover products. Following your suggestion, we further revised and improved this part of the manuscript. First, we further clarified the purpose of comparing OasisMap30 with other land cover products in the revised manuscript. The inclusion of MCD12Q1, ESA CCI LC, CLCD, and GLC_FCS30 was not intended merely for direct comparison among products with the same

spatial resolution, but also to examine how widely used datasets at multiple spatial scales perform in oasis regions. This helps to more comprehensively demonstrate the necessity of developing a land cover dataset for oases with high spatial and temporal resolution. As widely used and representative continuous land cover products, MCD12Q1 and ESA CCI LC still provide important comparative value. Therefore, we retained the comparison results for these two datasets to illustrate the differences among products at different spatial scales in describing land cover characteristics in oasis regions.

Meanwhile, we also carefully considered your suggestion regarding the appropriateness of the comparison datasets. Accordingly, in the revised manuscript, we additionally included the newly published annual 30 m land cover dataset for China, ALCC (1985–2022), and further analyzed the differences in performance between OasisMap30 and the relevant datasets. We believe that this addition helps strengthen the persuasiveness of same-resolution comparisons. The detailed revisions are as follows (Lines 188–192, 224–236, 292–294, Table S5, and Table S16–S19):

2.8 Datasets inter-comparison

We compared OasisMap30 with several widely used and well-validated land cover products, including three global datasets, namely MCD12Q1, ESACCI_LC, and GLC_FCS30, with spatial resolutions of 500, 300, and 30 m, respectively (Table S3). We also selected CLCD and ALCC, both of which are annual 30 m land cover datasets for China, with reported overall accuracies of 79.3% and 81.11%, respectively.

3.2 Comparison with existing Land cover datasets

Cross-dataset comparisons show that, for oasis regions in China, OasisMap30 exhibited substantially higher overall accuracy (93.64% in 2022) than CLCD (75.72%), ALCC (71.16%), GLC_FCS30 (74.13%), ESACCI_LC (66.22%) and MCD12Q1 (50.55%) (Table S6-S30). For each land cover category, OasisMap30 achieved higher and more stable F1 scores compared to datasets such as CLCD, ALCC, GLC_FCS30, and ESACCI_LC (Figure S3). OasisMap30 also showed a good ability to capture fine-scale details of oasis land cover (Figure 3). We further evaluated the accuracy of OasisMap30 using Geo-Wiki test samples (Table S31). The results showed that OasisMap30 achieves an overall accuracy of 74.36%, substantially higher than that of the other datasets (50.09–64.31%). For individual land cover classes, OasisMap30 also showed consistently higher classification accuracy than the five comparison datasets.

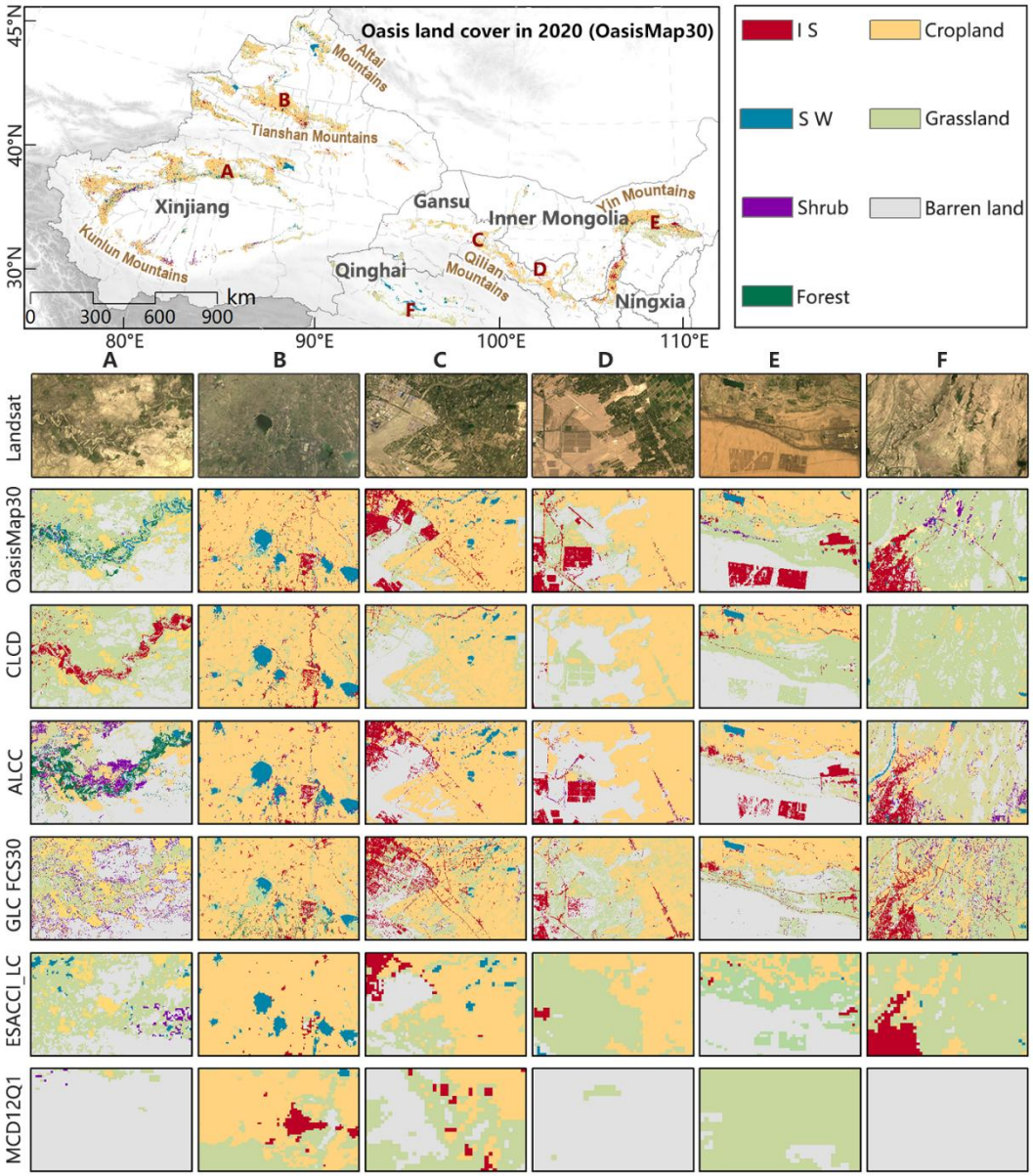

Figure 3: Regional comparison of oasis land-cover products. The first row shows Landsat imagery. The second to sixth rows show the spatial distribution of oasis land cover from OasisMap30 and five existing land-cover datasets. I S: Impervious surface; S W: Surface water. All the Landsat images are freely provided by USGS.

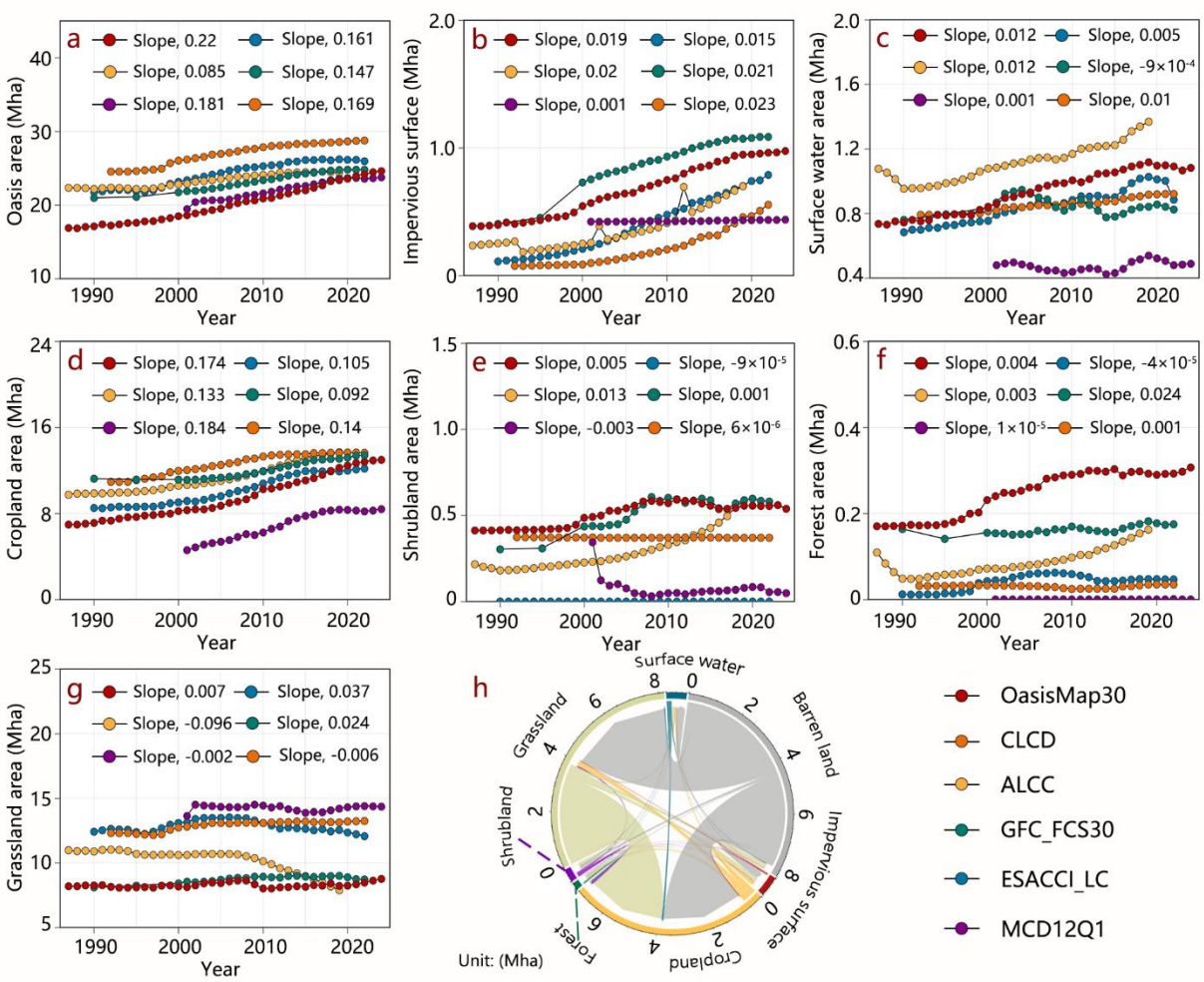

Figure 8: Comparison of temporal changes in different land cover areas of Chinese oases between OasisMap30 and various land cover datasets from 1987 to 2024 (a-g); Changes of seven land cover types during the period of 1987-2024 in oasis of China.

Table S4. Comparison of mapping accuracy, area, uncertainty based on visually interpreted for OasisMap30, CLCD, ALCC, GLC_FCS30, ESACCI_LC, and MCD12Q1.

Datasets	LUCC	1992		2002		2012		2022	
		UA (%)	Area (Mha)	UA (%)	Area (Mha)	UA (%)	Area (Mha)	UA (%)	Area (Mha)
OasisMap30	I S	83.65±6.6	0.41±0.042	87.85±5.89	0.6±0.045	87.93±4.59	0.8±0.05	90.86±4.08	0.96±0.051
	S W	90.37±4.25	0.75±0.047	90.28±4.09	0.9±0.049	93.93±3.14	1.01±0.041	93.66±2.91	1.09±0.047
	Cropland	93.3±1.09	7.33±0.137	93.52±1.00	8.38±0.131	93.18±0.95	10.5±0.141	95.76±0.68	12.81±0.133
	Shrubland	86.21±6.73	0.42±0.041	84.03±6.06	0.5±0.049	88.16±4.75	0.58±0.049	86.6±6.21	0.55±0.05
	Forest	87.18±9.67	0.17±0.027	88.1±9.19	0.25±0.031	86±9.1	0.3±0.035	88.24±8.31	0.29±0.034
	Grassland	90.02±1.21	8.16±0.149	90.85±1.17	8.27±0.145	91.6±1.14	8.11±0.144	91.78±1.13	8.48±0.134
	Barren land	89.32±1.29	8.08±0.144	90.08±1.35	6.43±0.132	90.08±1.67	4.02±0.109	90.61±2.54	1.12±0.063
CLCD	I S	20.19±6.15	0.12±0.04	42.06±7.29	0.25±0.075	44.25±5.89	0.52±0.078	47.43±5.36	0.79±0.184
	S W	82.54±5.2	0.7±0.084	85.41±4.77	0.81±0.082	84.12±4.77	0.91±0.085	82.94±4.38	0.89±0.142
	Cropland	94.58±0.91	8.56±0.26	93.38±0.97	9.11±0.243	93.73±0.85	11.34±0.329	90.7±0.93	12.17±0.324
	Shrubland	1.15±1.29	0±0.012	0.84±1.16	0±0.003	1.32±1.48	0±0.003	1.03±1.42	0±0.016
	Forest	7.69±7.24	0.01±0.013	2.38±1.74	0.04±0.029	8±5.01	0.05±0.021	7.84±5.22	0.05±0.067
	Grassland	63.07±1.6	12.64±0.471	72.66±1.51	13.4±0.477	71.55±1.62	12.67±0.492	63.08±1.71	12.07±0.709
	Barren land	64.54±1.83	18.77±0.438	60.42±2.02	17.18±0.447	62.56±2.46	15.29±0.464	59.61±3.02	14.84±0.692
ALCC	I S	62.5±7.54	0.4±0.069	61.68±8.32	0.78±0.084	71.26±6.07	0.97±0.084	88.57±3.38	1.09±0.184
	S W	88.56±3.81	0.76±0.103	91.36±3.3	0.92±0.108	88.79±3.66	0.85±0.113	94.05±2.34	0.83±0.293
	Cropland	96.65±0.71	11.23±0.25	96.06±0.74	11.15±0.241	96.06±0.68	12.28±0.3	87.89±1.04	13.42±0.396
	Shrubland	1.15±0.26	0.3±0.068	4.2±0.97	0.44±0.084	3.95±0.9	0.57±0.1	6.19±1	0.58±0.112
	Forest	7.69±5.12	0.16±0.023	21.43±9.03	0.15±0.031	22±8.74	0.16±0.032	19.61±6	0.18±0.077
	Grassland	54.83±1.62	8.11±0.421	61.36±1.67	8.5±0.431	59.95±1.76	8.88±0.469	47.69±1.78	8.72±0.604
	Barren land	59.06±1.87	18.07±0.407	62.71±1.99	17.1±0.417	60.23±2.34	15.31±0.463	62.88±2.74	14.24±0.651
GLC_FCS30	I S	41.35±6.21	0.4±0.091	71.03±6.73	0.78±0.119	76.44±5.56	0.97±0.088	72±5.6	1.09±0.14
	S W	77.72±5.83	0.76±0.077	77.3±5.25	0.92±0.125	82.72±4.86	0.85±0.097	71.04±5.34	0.83±0.103
	Cropland	94.19±0.92	11.23±0.272	91.13±1.09	11.15±0.263	93.14±0.9	12.28±0.294	93.42±0.79	13.42±0.294
	Shrubland	2.3±0.91	0.3±0.048	0.84±0.24	0.44±0.078	0.66±0.15	0.57±0.12	1.03±0.26	0.58±0.208
	Forest	30.77±6.53	0.16±0.069	21.43±5.26	0.15±0.064	18±4.93	0.16±0.053	27.45±7.43	0.18±0.049
	Grassland	57.83±1.69	8.11±0.398	61.55±1.68	8.5±0.416	64.42±1.69	8.88±0.486	52.97±1.81	8.72±0.657
	Barren land	67.09±1.78	18.07±0.395	66.71±1.85	17.1±0.418	55.5±2.29	15.31±0.472	60.26±2.7	14.24±0.66
ESACCI_LC	I S	24.04±7.26	0.08±0.03	37.38±8.37	0.11±0.034	50±7.15	0.24±0.035	66.86±5.93	0.55±0.094
	S W	77.11±5.5	0.79±0.095	81.09±5.04	0.83±0.092	74.3±5.52	0.86±0.08	73.02±4.96	0.92±0.142
	Cropland	81.45±1.39	10.96±0.401	86.49±1.18	12.12±0.385	88.37±1.06	13.45±0.371	82.03±1.16	13.64±0.442
	Shrubland	1.15±0.38	0.37±0.074	0.84±0.21	0.37±0.103	1.32±0.33	0.37±0.128	1.03±0.33	0.37±0.165
	Forest	5.13±4.9	0.03±0.021	2.38±1.88	0.03±0.031	2±2.24	0.03±0.027	1.96±1.7	0.04±0.023
	Grassland	46.06±1.49	12.31±0.457	47.55±1.53	12.92±0.455	52.86±1.66	13.17±0.472	49.86±1.61	13.26±0.636
	Barren land	50.44±1.71	16.26±0.435	51.26±1.88	14.42±0.416	60.86±2.33	12.69±0.416	48.25±2.74	12.02±0.591
MCD12Q1	I S	/	/	14.95±2.95	0.42±0.095	13.79±2.6	0.43±0.081	20±3.15	0.44±0.112
	S W	/	/	24.87±4.69	0.49±0.091	26.64±4.74	0.46±0.095	34.53±5.48	0.48±0.1
	Cropland	/	/	35.19±1.67	4.86±0.274	43.63±1.63	6.79±0.317	53.76±1.53	8.19±0.404
	Shrubland	/	/	0.84±0.42	0.12±0.044	1.32±0.85	0.04±0.038	3.09±1.89	0.06±0.091
	Forest	/	/	2.38±4.61	0.001±0.013	2±2.74	0.001±0.019	3.92±5.33	0.001±0.013
	Grassland	/	/	49.46±1.24	14.51±0.524	53.64±1.34	14.4±0.543	51.89±1.36	14.41±0.707
	Barren land	/	/	51.09±1.55	17.36±0.515	63.54±1.82	15.63±0.533	57.64±2.11	14.18±0.707

Note: 95% confidence intervals were used to estimate uncertainty. I S: Impervious surface; S W: Surface water.

Table S15. Confusion matrix of ALCC in 1992 based on visually-interpreted test samples.

Ground Reference	Classification							Sum	UA (%)
	I S	S W	Cropland	Shrubland	Forest	Grassland	Barren land		
I S	65	2	19	1	0	10	7	104	62.50
S W	0	147	5	0	0	9	5	166	88.55
Cropland	9	3	1730	0	0	43	5	1790	96.65
Shrub	3	3	39	1	1	39	1	87	1.15
Forest	2	1	23	0	3	8	2	39	7.69
Grassland	19	67	469	68	5	1170	336	2134	54.83
Barren land	2	16	107	3	0	708	1206	2042	59.06
Sum	100	239	2392	73	9	1987	1562	6362	Kappa=0.55
PA (%)	65.00	61.51	72.32	1.37	33.33	58.88	77.21		OA=67.93%

Note: I S: Impervious surface; S W: Surface water.

Table S16. Confusion matrix of ALCC in 2002 based on visually-interpreted test samples.

Ground Reference	Classification							Sum	UA (%)
	I S	S W	Cropland	Shrubland	Forest	Grassland	Barren land		
I S	66	0	14	0	0	22	5	107	61.68
S W	0	169	6	0	0	3	7	185	91.35
Cropland	7	3	2047	0	1	67	6	2131	96.06
Shrub	0	10	38	5	2	57	7	119	4.20
Forest	0	0	19	3	9	11	0	42	21.43
Grassland	7	57	373	53	6	1315	332	2143	61.36
Barren land	2	16	70	9	0	538	1068	1703	62.71
Sum	82	255	2567	70	18	2013	1425	6430	Kappa=0.61
PA (%)	80.49	66.27	79.74	7.14	50.00	65.33	74.95		OA=72.77%

Note: I S: Impervious surface; S W: Surface water.

Table S17. Confusion matrix of ALCC in 2012 based on visually-interpreted test samples.

Ground Reference	Classification							Sum	UA (%)
	I S	S W	Cropland	Shrubland	Forest	Grassland	Barren land		
I S	124	1	14	0	0	26	9	174	71.26
S W	0	190	7	0	0	8	9	214	88.79
Cropland	8	3	2437	0	2	81	6	2537	96.06
Shrub	1	7	38	6	2	85	13	152	3.95
Forest	0	3	17	3	11	15	1	50	22.00
Grassland	19	40	406	55	5	1235	300	2060	59.95
Barren land	1	11	81	8	0	344	674	1119	60.23
Sum	153	255	3000	72	20	1794	1012	6306	Kappa=0.62
PA (%)	81.05	74.51	81.23	8.33	55.00	68.84	66.60		OA=74.17%

Note: I S: Impervious surface; S W: Surface water.

Table S18. Confusion matrix of ALCC in 2022 based on visually-interpreted test samples.

Ground Reference	Classification							Sum	UA (%)
	I S	S W	Cropland	Shrubland	Forest	Grassland	Barren land		
I S	155	1	9	0	0	5	5	175	88.57
S W	2	237	4	0	0	3	6	252	94.05
Cropland	76	4	2817	5	8	270	25	3205	87.89
Shrub	1	5	32	6	5	41	7	97	6.19
Forest	4	5	21	0	10	10	1	51	19.61
Grassland	58	96	396	126	10	1010	422	2118	47.69
Barren land	6	22	31	1	1	109	288	458	62.88
Sum	302	370	3310	138	34	1448	754	6356	Kappa=0.56
PA (%)	51.32	64.05	85.11	4.35	29.41	69.75	38.20		OA=71.16%

Note: I S: Impervious surface; S W: Surface water.

Specific comments

[RC #2 Specific comments 1]

Figure 2, the table overlays with map.

[Response]

We thank the reviewer for pointing out this issue. We have adjusted the layout of Figure 2 in the latest version to avoid the overlap between the table and the map. The detailed revisions are as follows:

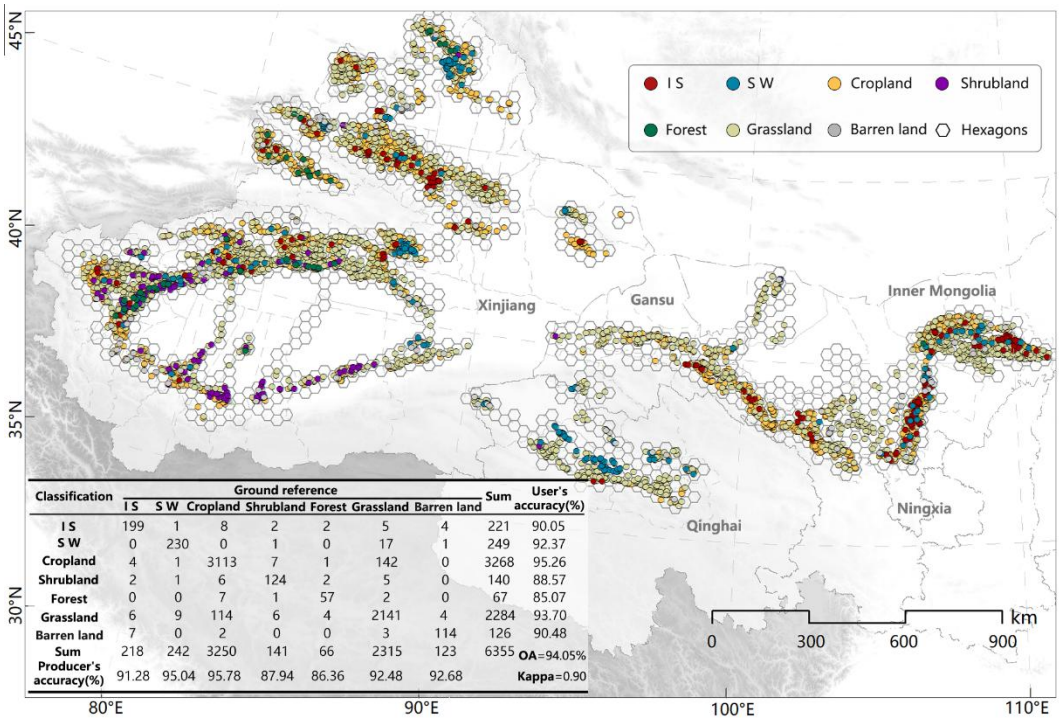

Classification	Ground reference							Sum	User's accuracy(%)
	I S	S W	Cropland	Shrubland	Forest	Grassland	Barren land		
I S	199	1	8	2	2	5	4	221	90.05
S W	0	230	0	1	0	17	1	249	92.37
Cropland	4	1	3113	7	1	142	0	3268	95.26
Shrubland	2	1	6	124	2	5	0	140	88.57
Forest	0	0	7	1	57	2	0	67	85.07
Grassland	6	9	114	6	4	2141	4	2284	93.70
Barren land	7	0	2	0	0	3	114	126	90.48
Sum	218	242	3250	141	66	2315	123	6355	OA=94.05%
Producer's accuracy(%)	91.28	95.04	95.78	87.94	86.36	92.48	92.68		Kappa=0.90

Figure 2: Accuracy assessment of the OasisMap30 dataset based on visually interpreted samples (taking the year 2024 as an example). I S: Impervious surface; S W: Surface water.

[RC #2 Specific comments 2]

In figure S2, there are errors in label of X axis.

[Response]

We thank the reviewer for pointing out this issue. The errors in the x-axis labels of Figure S2 have been corrected in the latest version. The detailed revisions are as follows:

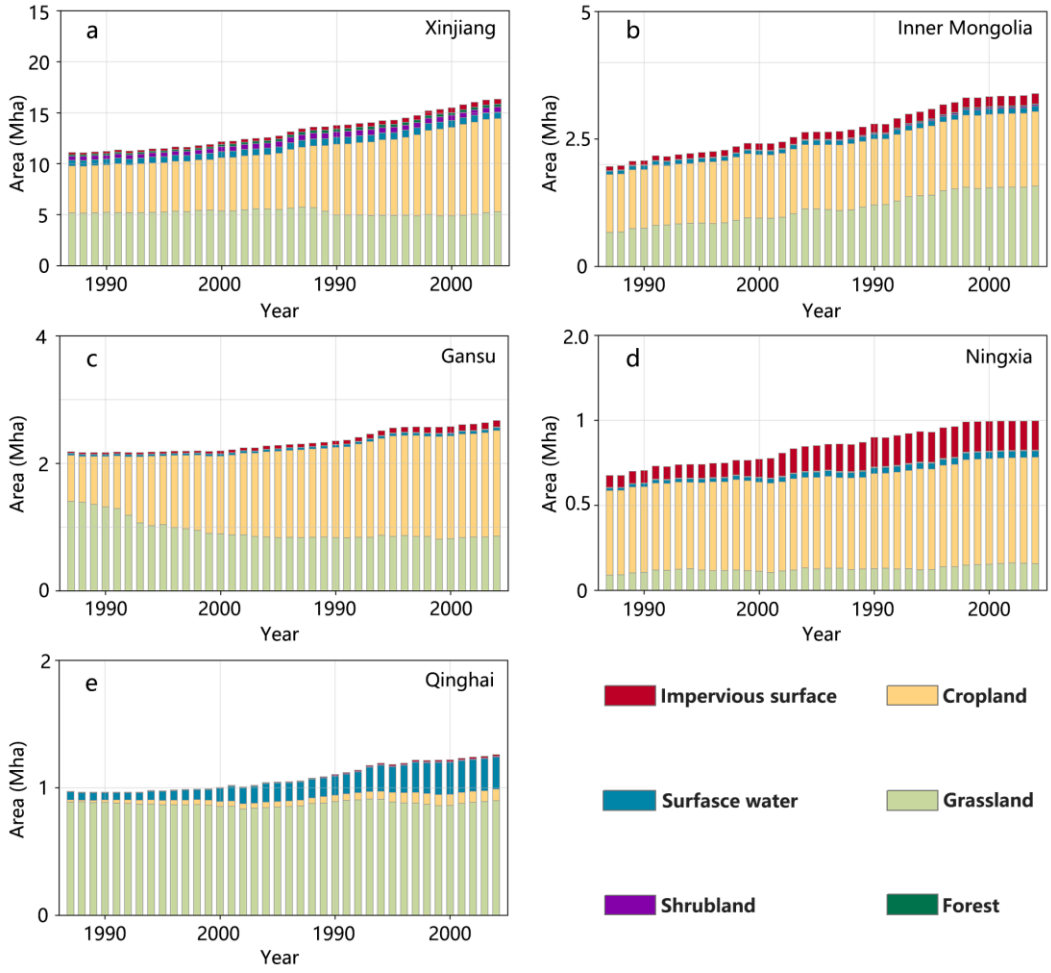

Figure S5: Changes in the spatial structure of oases at provincial/autonomous scales during 1987–2024.

[RC #2 Specific comments 3]

In line 80-81, the remark "we manually inspected the imagery and masked out mountain regions and clearly unvegetated deserts (e.g., the Taklamakan Desert)" is not consistent to the data described in the next sections and the supplement. Oasis in the Taklamakan Desert also were mapped.

[Response]

We thank the reviewer for this valuable comment. The previous wording may have caused misunderstanding. In the revised manuscript, we removed the specific example and clarified that only clearly unvegetated desert areas outside oasis landscapes were masked out, while

oasis areas within desert regions were retained for subsequent classification. The detailed revisions are as follows (Lines 92–94):

On this basis, we manually inspected the imagery and masked out mountain regions and clearly unvegetated desert areas, while retaining oasis areas within desert regions, and then delineated the final study area for classification on the GEE platform.

[RC #2 Specific comments 4]

As illustrated in Figure 2 and 3, the legend non-oasis is not reasonable. According to the definition of oasis, fragmented barren areas within an oasis are elements of oasis. I suggest a modification of the relevant figures.

[Response]

We thank the reviewer for pointing out this issue. In the revised manuscript, we replaced the label “non-oasis” with “barren land” in Figures 2 and 3 to make the figure legends more precise and consistent with the land-cover classification system used in this study. The detailed revisions are as follows:

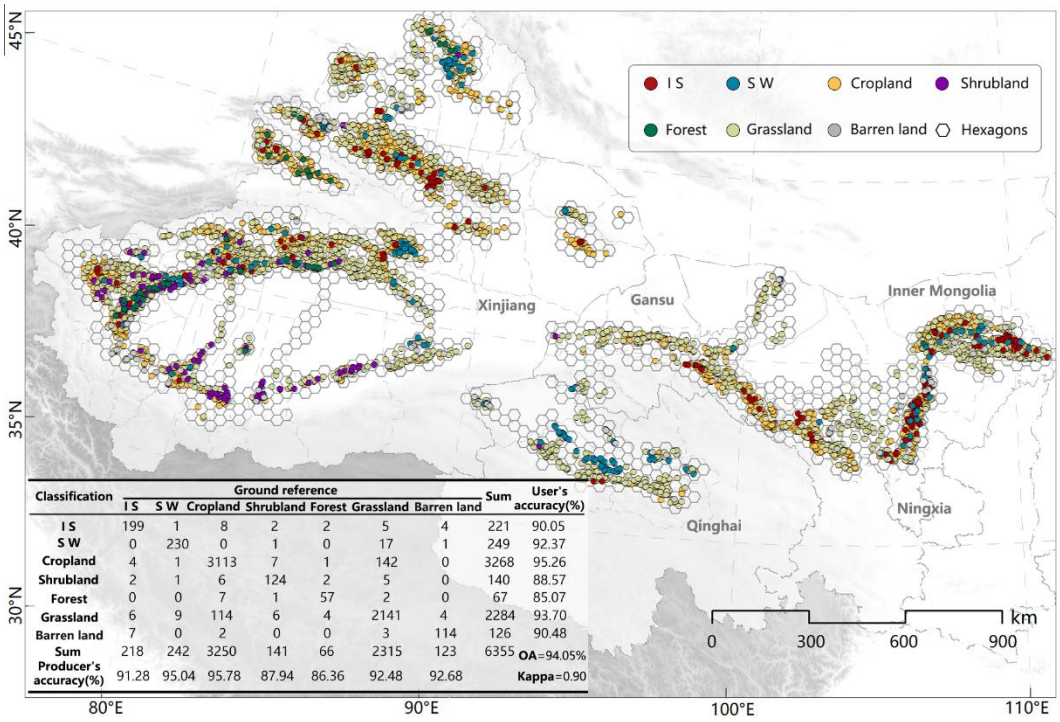

Classification	Ground reference							Sum	User's accuracy(%)
	I S	S W	Cropland	Shrubland	Forest	Grassland	Barren land		
I S	199	1	8	2	2	5	4	221	90.05
S W	0	230	0	1	0	17	1	249	92.37
Cropland	4	1	3113	7	1	142	0	3268	95.26
Shrubland	2	1	6	124	2	5	0	140	88.57
Forest	0	0	7	1	57	2	0	67	85.07
Grassland	6	9	114	6	4	2141	4	2284	93.70
Barren land	7	0	2	0	0	3	114	126	90.48
Sum	218	242	3250	141	66	2315	123	6355	OA=94.05%
Producer's accuracy(%)	91.28	95.04	95.78	87.94	86.36	92.48	92.68		Kappa=0.90

Figure 2: Accuracy assessment of the OasisMap30 dataset based on visually interpreted samples (taking the year 2024 as an example). I S: Impervious surface; S W: Surface water.

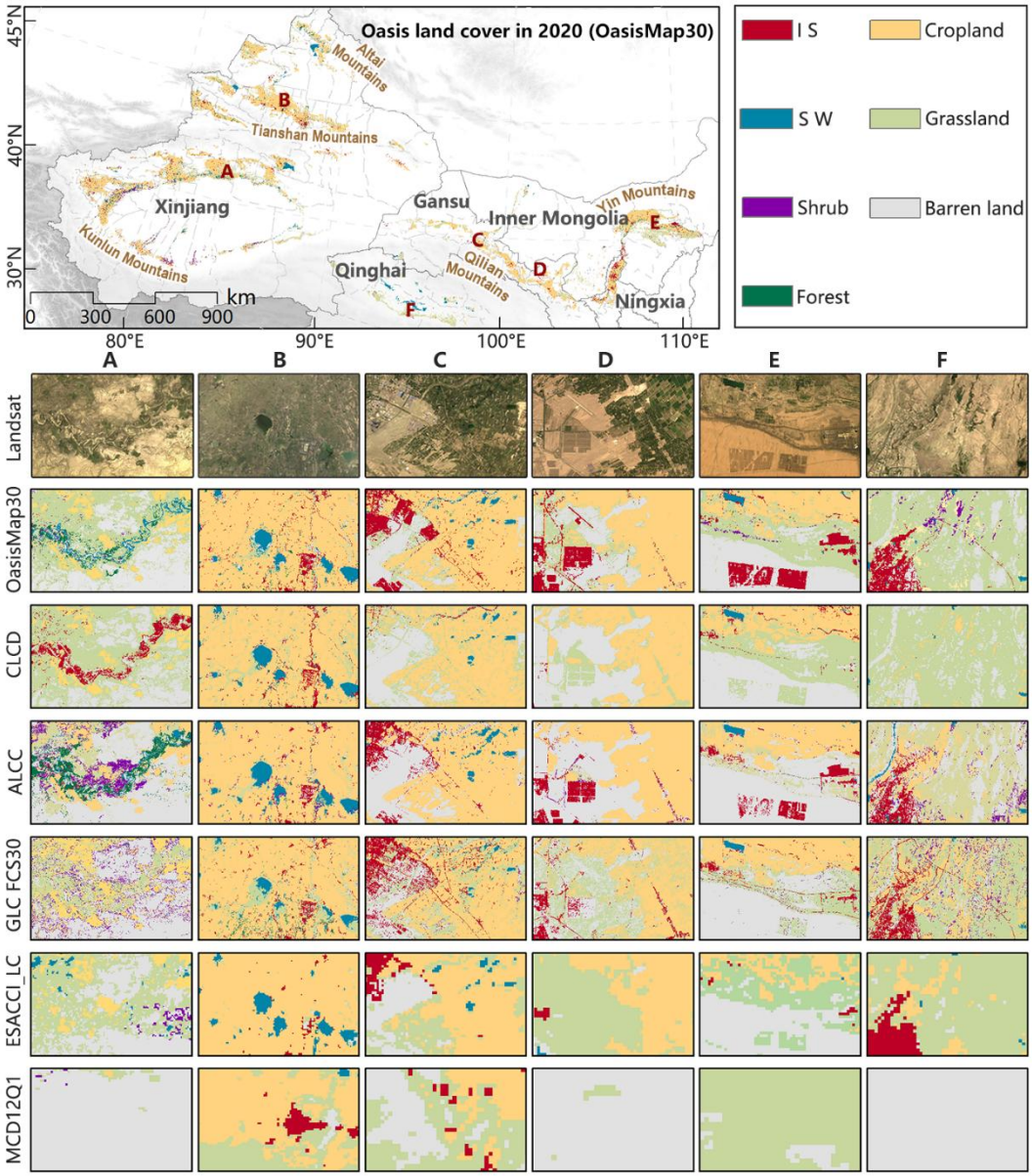

Figure 3: Regional comparison of oasis land-cover products. The first row shows Landsat imagery. The second to sixth rows show the spatial distribution of oasis land cover from OasisMap30 and five existing land-cover datasets. I S: Impervious surface; S W: Surface water. All the Landsat images are freely provided by USGS.

[RC #2 Specific comments 5]

In Figure 3, the dashed lines were used to show the mountains. However, mountains also areas. To avoid the misunderstanding of readers, change the symbols of mountains. For instance, only keep the text labels.

[Response]

We thank the reviewer for this helpful suggestion. Following your suggestion, we removed the dashed lines used to indicate the mountains in Figure 3 and retained only the text labels to avoid possible misunderstanding. The detailed revisions are as follows:

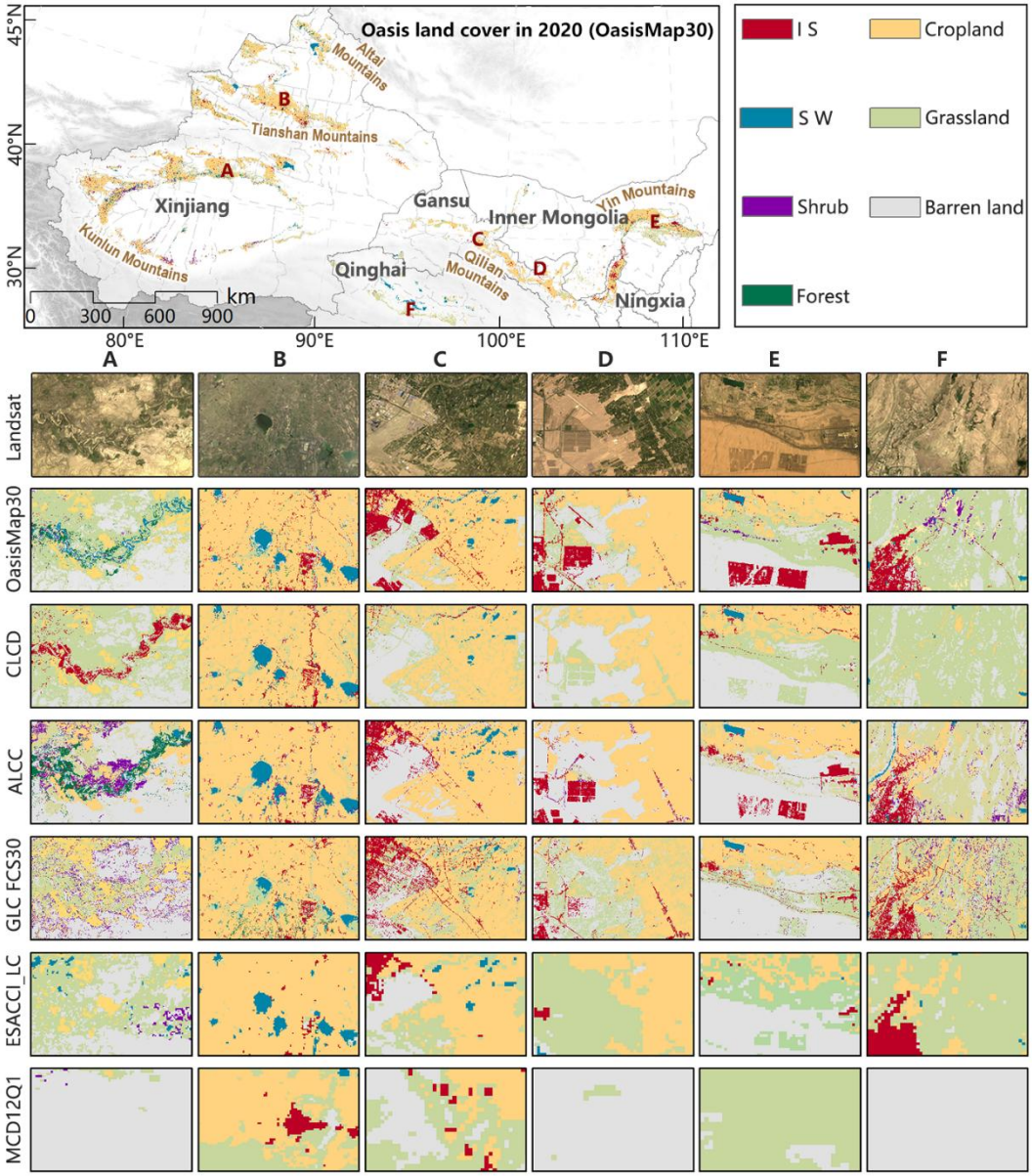

Figure 3: Regional comparison of oasis land-cover products. The first row shows Landsat imagery. The second to sixth rows show the spatial distribution of oasis land cover from OasisMap30 and five existing land-cover datasets. I S: Impervious surface; S W: Surface water. All the Landsat images are freely provided by USGS.

Response to RC#3

***To RC #3*:**

Thank you for your very professional and thoughtful comments. We have followed all your suggestions in our revision. Below are the Reviewer's previous comments, followed by our responses.

***RC #3's*:**

General comments

[RC #3's General comments]

High spatio-temporal resolution maps of oasis land cover are valuable for understanding ecological and societal development processes in dryland regions. It is an interesting work on high-spatio-temporal resolution oasis mapping, which can enhance studies on oasis landscape pattern and sustainable development of oasis region.

[Response]

Thank you for your positive comment.

[RC #3 General comments 1]

1. The scientific question of this study should be reorganized and rewritten for more clear and specific, especially for mapping techniques and methods on oasis data.

[Response]

We thank the reviewer for this valuable comment. Following your suggestion, we further reorganized and revised the Introduction and Methods sections. In the Introduction, we refined the scientific question of this study and explicitly identified accurate detection of land-cover change and control of error propagation in long-term annual oasis mapping as the key scientific issue. In the Methods section, we further clarified the technical workflow for oasis land-cover

mapping, including feature-space construction, sample selection and partitioning, random forest classification, annual land-cover mapping based on the LandTrendr–PCA framework, and accuracy assessment using visually interpreted and third-party test samples. These revisions have made the scientific question, technical workflow, and methodological logic of the study clearer and more specific. The detailed revisions are as follows (Lines 78–87, 106–128, and 136–142):

1 Introduction

The integration of these two methods provides a potential way to improve the reliability of annual land-cover mapping. However, in oasis regions with complex landscape patterns and strong interannual variability, accurately capturing land-cover changes and limiting error propagation remain key challenges for achieving long-term land-cover mapping at high spatial and temporal resolution.

In this study, we developed a new framework for annual land-cover mapping at fine resolution by combining random forest classification with the LandTrendr algorithm and principal component analysis. Based on this framework, we integrated multi-source remote sensing data to produce an annual 30 m resolution land cover dataset for Chinese oases (OasisMap30) from 1987 to 2024. We further assessed the accuracy of OasisMap30 using visually interpreted and third-party test samples, evaluated its performance through inter-comparison with existing land-cover and thematic datasets, and investigated the long-term dynamics of land-cover change in China's oases over the past four decades.

2.3 Feature space construction

Based on Landsat imagery and SRTM DEM data, we derived the predictor variables used in the random forest classification (Breiman, 2001). Among these, slope, aspect, and hillshade were computed from the DEM data. To enhance classification performance, we further applied the tasseled cap transformation to derive brightness, greenness, and wetness components (Crist, 1985; Huang et al., 2002; Baig et al., 2014). The final feature indicators comprise four categories: spectral features, terrain features, tasseled-cap transform, and gray-level co-occurrence matrix. The detailed variables used in the classification are listed in Table 1.

Table1. Independent variables of the random forest model for land-cover classification.

Feature indicators	Independent variables
Spectral feature	ρ_{Blue}, ρ_{Green}, ρ_{Red}, ρ_{Nir}, ρ_{SWIR1}, ρ_{SWIR2}, Normalized difference vegetation index (NDVI), Modified normalized difference water index (MNDWI), Normalized difference built-up index (NDBI)
Terrain feature	Elevation, Slope, Aspect, Hillshade
Tasseled-cap transform	Wetness index, Brightness index, Greenness index
Gray-level co-occurrence matrix	Entropy, Correlation, Variance, Contrast, Angular second moment, Inverse difference moment

Note: ρ_{Blue}, ρ_{Green}, ρ_{Red}, ρ_{Nir}, ρ_{SWIR1}, ρ_{SWIR2} are the surface reflectance values in the blue, green, red, near infrared, shortwave infrared 1, and 2 bands of the Landsat image, respectively.

2.4 Land-cover classification

We used a random forest algorithm for land-cover classification (Figure 1). Landsat images were first imported into GEE and pre-processed, including cloud and snow masking and mosaicking. Visually interpreted samples for different land-cover types were then collected based on the pre-processed Landsat imagery in combination with Google Earth historical imagery. To ensure a spatially uniform distribution of samples across the oasis region, the oasis area was divided into approximately 1100 independent units using regular hexagons with a 10 km side length, and 25 sample points were randomly generated within each unit. After visual interpretation and quality screening, at least 27000 samples were retained for each year (Figure S1).

For each sample, the predictor variables described in Section 2.3 were extracted from the annual Landsat image composites and SRTM DEM, including spectral features, terrain features, tasseled-cap components, and gray-level co-occurrence matrix features (Table 1). The calculation methods for each indicator are detailed in Supplementary Table 1. The samples were then divided into training and validation subsets at a ratio of 7:3. The training subset was used to train the random forest classifier, whereas the validation subset was used to assess classification performance. The trained classifier was then applied to the Landsat image composites to generate the initial land-cover maps.

…

2.5 LandTrendr–PCA based annual land-cover mapping

Land-cover classification is prone to error propagation, especially when producing annual map series, where classification errors can accumulate over time. Employing the LandTrendr algorithm to identify areas exhibiting abrupt changes in surface reflectance, followed by machine learning classification of these areas, can effectively reduce the impact of error propagation. Therefore, to map land-cover dynamics from 1987 to 2024 while limiting the propagation of classification errors, we used the final 2024 oasis land-cover dataset as the baseline map and applied the LandTrendr algorithm to the annual time series of spectral indices, with the main parameter settings provided in Supplementary Table 2.

[RC #3 General comments 2]

2. How the random forest model on land-cover classification used in this study, how to get the independent variables?

[Response]

We thank the reviewer for raising this important question. In the revised manuscript, we have further clarified how the random forest classifier was used for land-cover classification and

how the independent variables were obtained. Specifically, we revised Sections 2.3 and 2.4 to explain that the predictor variables were derived from annual Landsat image composites and SRTM DEM data, and that their detailed definitions and calculation methods are provided in Table 1 and Supplementary Table 1. We also clarified the generation of visually interpreted samples, the ratio used to divide the samples into training and validation subsets, and the specific workflow of the random forest classification. The detailed revisions are as follows (Lines 106–128 and Table S1):

2.3 Feature space construction

Based on Landsat imagery and SRTM DEM data, we derived the predictor variables used in the random forest classification (Breiman, 2001). Among these, slope, aspect, and hillshade were computed from the DEM data. To enhance classification performance, we further applied the tasseled cap transformation to derive brightness, greenness, and wetness components (Crist, 1985; Huang et al., 2002; Baig et al., 2014). The final feature indicators comprise four categories: spectral features, terrain features, tasseled-cap transform, and gray-level co-occurrence matrix. The detailed variables used in the classification are listed in Table 1.

Table1. Independent variables of the random forest model for land-cover classification.

Feature indicators	Independent variables
Spectral feature	ρ_{Blue}, ρ_{Green}, ρ_{Red}, ρ_{Nir}, ρ_{SWIR1}, ρ_{SWIR2}, Normalized difference vegetation index (NDVI), Modified normalized difference water index (MNDWI), Normalized difference built-up index (NDBI)
Terrain feature	Elevation, Slope, Aspect, Hillshade
Tasseled-cap transform	Wetness index, Brightness index, Greenness index
Gray-level co-occurrence matrix	Entropy, Correlation, Variance, Contrast, Angular second moment, Inverse difference moment

Note: ρ_{Blue}, ρ_{Green}, ρ_{Red}, ρ_{Nir}, ρ_{SWIR1}, ρ_{SWIR2} are the surface reflectance values in the blue, green, red, near infrared, shortwave infrared 1, and 2 bands of the Landsat image, respectively.

2.4 Land-cover classification

We used a random forest algorithm for land-cover classification (Figure 1). Landsat images were first imported into GEE and pre-processed, including cloud and snow masking and mosaicking. Visually interpreted samples for different land-cover types were then collected based on the pre-processed Landsat imagery in combination with Google Earth historical imagery. To ensure a spatially uniform distribution of samples across the oasis region, the oasis area was divided into approximately 1100 independent units using regular hexagons with a 10 km side length, and 25 sample points were randomly generated within each unit. After visual interpretation and quality screening, at least 27000 samples were retained for each year (Figure S1).

For each sample, the predictor variables described in Section 2.3 were extracted from the annual Landsat image composites and SRTM DEM, including spectral features, terrain features, tasseled-cap components, and gray-level co-occurrence matrix features (Table 1). The calculation methods for each indicator are

detailed in Supplementary Table 1. The samples were then divided into training and validation subsets at a ratio of 7:3. The training subset was used to train the random forest classifier, whereas the validation subset was used to assess classification performance. The trained classifier was then applied to the Landsat image composites to generate the initial land-cover maps.

Table S1. The features used for OasisMap30 mapping.

Features	Description
ρ_{Blue}, ρ_{Green}, ρ_{Red}, ρ_{Nir}, ρ_{SWI1}, ρ_{SWI2}	50th percentile value of surface reflectance derived from all available Landsat image.
NDVI	$NDVI = (\rho_{Nir} - \rho_{Red}) / (\rho_{Nir} + \rho_{Red})$
MNDWI	$MNDWI = (\rho_{Green} - \rho_{SWI1}) / (\rho_{Green} + \rho_{SWI1})$
NDBI	$NDBI = (\rho_{SWI1} - \rho_{Nir}) / (\rho_{SWI1} + \rho_{Nir})$
Wetness	for Landsat 5 TM: $Wetness = 0.1509 \times \rho_{Blue} + 0.1973 \times \rho_{Green} + 0.3279 \times \rho_{Red} + 0.3406 \times \rho_{Nir} - 0.7112 \times \rho_{SWI1} - 0.4572 \times \rho_{SWI2}$ for Landsat 7 ETM+: $Wetness = 0.2626 \times \rho_{Blue} + 0.2141 \times \rho_{Green} + 0.0926 \times \rho_{Red} + 0.0656 \times \rho_{Nir} - 0.7629 \times \rho_{SWI1} - 0.5388 \times \rho_{SWI2}$ for Landsat 8 OLI: $Wetness = 0.1511 \times \rho_{Blue} + 0.1973 \times \rho_{Green} + 0.3283 \times \rho_{Red} + 0.3407 \times \rho_{Nir} - 0.7117 \times \rho_{SWI1} - \times 0.4559 \rho_{SWI2}$
Soil brightness	for Landsat 5 TM: $Soil\ brightness = 0.3037 \times \rho_{Blue} + 0.2793 \times \rho_{Green} + 0.4743 \times \rho_{Red} + 0.5585 \times \rho_{Nir} + 0.5082 \times \rho_{SWI1} + 0.1863 \times \rho_{SWI2}$ for Landsat 7 ETM+: $Soil\ brightness = 0.3561 \times \rho_{Blue} + 0.3972 \times \rho_{Green} + 0.3904 \times \rho_{Red} + 0.6966 \times \rho_{Nir} + 0.2286 \times \rho_{SWI1} + 0.1596 \times \rho_{SWI2}$ for Landsat 8 OLI: $Soil\ brightness = 0.3029 \times \rho_{Blue} + 0.2786 \times \rho_{Green} + 0.4733 \times \rho_{Red} + 0.5599 \times \rho_{Nir} + 0.508 \times \rho_{SWI1} + 0.1872 \times \rho_{SWI2}$
Greenness	for Landsat 5 TM: $Greenness = -0.2848 \times \rho_{Blue} - 0.243 \times \rho_{Green} - 0.5436 \times \rho_{Red} + 0.7243 \times \rho_{Nir} + 0.0840 \times \rho_{SWI1} - 0.1800 \times \rho_{SWI2}$ for Landsat 7 ETM+: $Greenness = -0.3344 \times \rho_{Blue} - 0.3544 \times \rho_{Green} - 0.4556 \times \rho_{Red} + 0.6966 \times \rho_{Nir} - 0.0242 \times \rho_{SWI1} - 0.2630 \times \rho_{SWI2}$ for Landsat 8 OLI: $Greenness = -0.2941 \times \rho_{Blue} - 0.243 \times \rho_{Green} + 0.5424 \times \rho_{Red} + 0.7276 \times \rho_{Nir} + 0.0713 \times \rho_{SWI1} - 0.1608 \times \rho_{SWI2}$
Elevation, Slope, Aspect, and Hillshade	Elevation, Slope, Aspect, and Hillshade calculated from SRTM elevation.

[RC #3 General comments 3]

3. More discussion should be added, on the methodological techniques, innovation, novelty, also the significance.

[Response]

We thank the reviewer for this valuable suggestion. Following your comment, we have strengthened the discussion in the revised manuscript. Specifically, we added a new section,

"4.2 Value and potential applications of OasisMap30", to further discuss the methodological strengths of the proposed framework, its novelty in long-term oasis land-cover mapping, and the significance and potential applications of OasisMap30. The detailed revisions are as follows (Lines 323–338):

4.2 Value and potential applications of OasisMap30

This study developed a long-term, high-spatial-resolution land-cover dataset for Chinese oases based on an annual mapping framework for oasis regions. Compared with existing continuous land-cover products, OasisMap30 has several clear advantages for long-term oasis mapping. the 30 m spatial resolution enables it to better capture fragmented land-cover patterns in oasis regions. Within oases, cropland, grassland, surface water, impervious surfaces, and barren land are often form a complex mosaic, making it difficult for coarse-resolution products to accurately characterize fine-scale land-cover patterns (Yang and Huang, 2021). Meanwhile, the LandTrendr–PCA based disturbance detection framework can help reduce error propagation in long-term high-spatio-temporal-resolution mapping. The LandTrendr–PCA method integrates surface disturbance signals from multiple indicators, thereby reducing error propagation during annual mapping (Mugiraneza et al., 2020). By combining random forest classification with this method, temporal consistency can be improved while preserving spatial detail. Therefore, this framework is therefore particularly suitable for oasis regions, where land-cover changes are substantial and landscape patterns are complex.

Overall, OasisMap30 shows strong capability in capturing land-cover changes. The dataset provides fundamental data for studies on oasis expansion, land-cover transitions, and their eco-hydrological effects, and also provides valuable support for research on human-environment relationships, the water-food-ecosystem nexus, and environmental sustainability in oasis regions.

Reference

Mugiraneza, T., Nascetti, A., and Ban, Y.: Continuous Monitoring of Urban Land Cover Change Trajectories with Landsat Time Series and LandTrendr-Google Earth Engine Cloud Computing, Remote Sensing, 12, 2883, https://doi.org/10.3390/rs12182883, 2020.

Yang, J. and Huang, X.: The 30 m annual land cover dataset and its dynamics in China from 1990 to 2019, Earth Syst. Sci. Data, 13, 3907–3925, https://doi.org/10.5194/essd-13-3907-2021, 2021.